# Statistically downscaling from an Earth System Model of Intermediate Complexity to reconstruct past climate gradients across the UK

Mark Hoar
Jean Palutikof

Climatic Research Unit
University of East Anglia

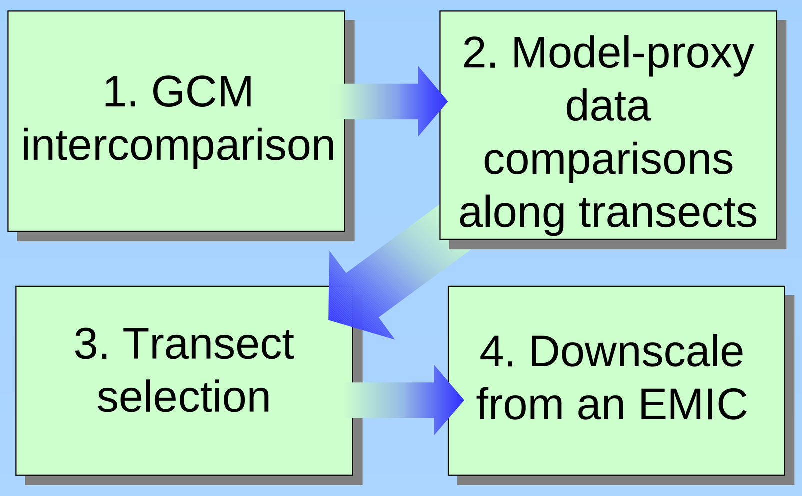


**Figure 1** The downscaling process

## Introduction

Earth System Models of Intermediate Complexity (EMICs) have the advantage of allowing transient experiments over long periods of time. Here we present a method of reconstructing gradients of climate across the UK during the last glacial interglacial using the output from such models.

A statistical downscaling procedure is used, with four parts (**Figure 1**):

(i) Statistical methods are used to compare the output from 20 models of the Palaeoclimate Modelling Intercomparison Project (PMIP) and 7 sensitivity studies for the study area shown in **Figure 2**. The analysis is done for the present day, the mid-Holocene and the Last Glacial Maximum for the months of January, April, July and October.

(ii) Comparisons of model output with observed and proxy data sets are made along 4 transects (**Figure 2**) and k-means cluster analysis is used to determine a best model.

(iii) Statistical comparisons are then made to choose a best transect for each time period that can be used in a downscaling method.

(iv) Finally, model output from the Université Catholique de Louvain (UCL) is downscaled to reconstruct surface air temperature over the last 126 kyr BP.

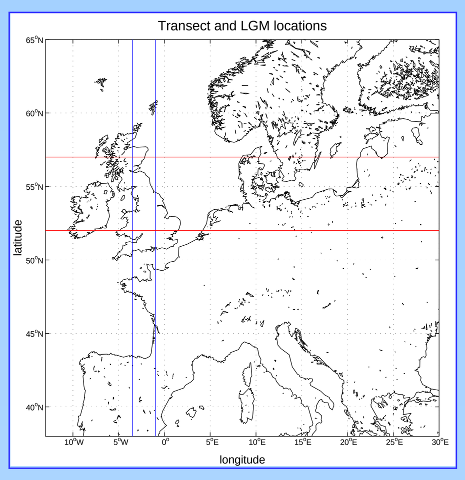


**Figure 2** Spatial domain of study area and transects

## 1. GCM intercomparison

After interpolating the models onto a common grid, correlation matrices (containing Spearman ranked correlation coefficients) are produced for each month of each time slice (**Table 1**). Hierarchical cluster analysis is applied to each matrix to gain a more detailed understanding of the relationships between the models (**Figure 3**).

| | January | | | P = PMIP | S = Sensitivity study | | | | |
|---|---|---|---|---|---|---|---|---|---|
| | ccc(P) | ccm1(P) | gen1(P) | gen2(P) | gfdl(P) | mri(P) | ugamp(P) | hadam2(P) | mri21k(S) |
| ccc(P) | **1.00** | 0.86 | 0.68 | 0.95 | 0.86 | 0.93 | 0.89 | 0.97 | 0.96 |
| ccm1(P) | 0.86 | **1.00** | 0.89 | 0.93 | 0.94 | 0.95 | 0.97 | 0.85 | 0.88 |
| gen1(P) | 0.68 | 0.89 | **1.00** | 0.80 | 0.93 | 0.83 | 0.92 | 0.66 | 0.70 |
| gen2(P) | 0.95 | 0.93 | 0.80 | **1.00** | 0.94 | 0.98 | 0.96 | 0.93 | 0.96 |
| gfdl(P) | 0.86 | 0.94 | 0.93 | 0.94 | **1.00** | 0.95 | 0.99 | 0.84 | 0.88 |
| mri(P) | 0.93 | 0.95 | 0.83 | 0.98 | 0.95 | **1.00** | 0.97 | 0.93 | 0.96 |
| ugamp(P) | 0.89 | 0.97 | 0.92 | 0.96 | 0.99 | 0.97 | **1.00** | 0.88 | 0.91 |
| hadam2(P) | 0.97 | 0.85 | 0.66 | 0.93 | 0.84 | 0.93 | 0.88 | **1.00** | 0.96 |
| mri21k(S) | 0.96 | 0.88 | 0.70 | 0.96 | 0.88 | 0.96 | 0.91 | 0.96 | **1.00** |

**Table 1** Correlation matrix for 21 kyr BP surface air temperature with fixed SSTs

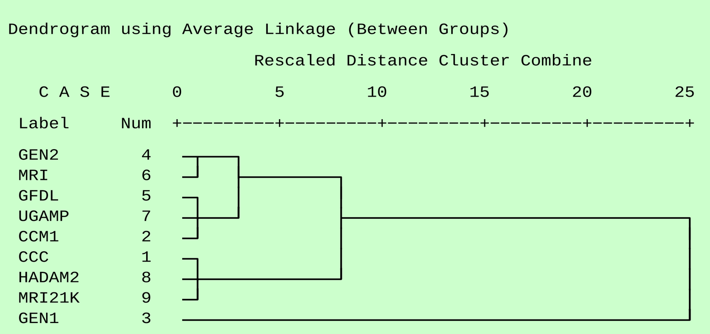


**Figure 3** Dendrogram showing the results of the hierarchical cluster analysis for table 1.

**Correlation matrices:**

- Correlation coefficients are higher for temperature than for precipitation.
- Correlation coefficients are large and positive for the absolute time slice matrices, but were variable (positive and negative) when calculated from 6 kyr BP minus present day values.

Results from cluster analysis of matrices

- The post-PMIP Sensitivity studies do not cluster together.
- LMD4, GENESIS1 and CCM1 often resisted forming clusters with the other models.
- Related models from the same institute would often cluster together.
- There are no temporally consistent cluster patterns.

Q1 Do sensitivity studies cluster together?

Q2 Do any models resist forming clusters?

Q3. Do related models cluster together?

Q4. Are there any consistent cluster patterns?

## 2. Model-proxy data comparisons along transects

For the present day and mid-Holocene slices (**Figure 4**), the transects from the model ensemble were compared with the New *et al*. (1999) 0.5° observed temperature data set, and the proxy pollen data set of Cheddadi *et al*. (1997) respectively. Comparisons were made statistically using four parameters: correlation coefficients with and without the linear trend removed, and root mean square error with and without the linear trend removed. For the Last Glacial Maximum, only spot comparisons could be made visually (**Figures 5 and 6**).

For the present day, k-means cluster analysis showed that the model that best reproduced the New *et al*. (1999) observed data set was different for each transect and month (**Table 2**).

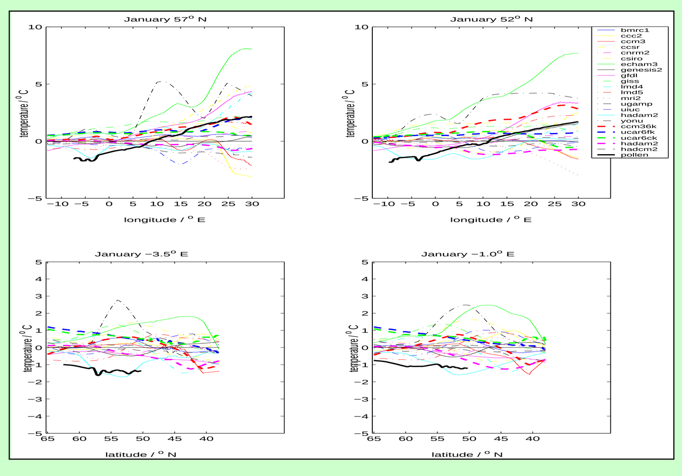


**Figure 4** Model temperature data vs Cheddadi *et al*. (1997) for 6-0 kyr BP.

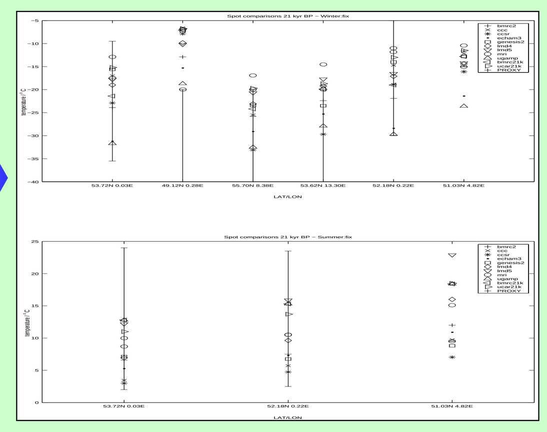

**Figure 5** Model-proxy comparisons for 21 kyr BP January temperature.

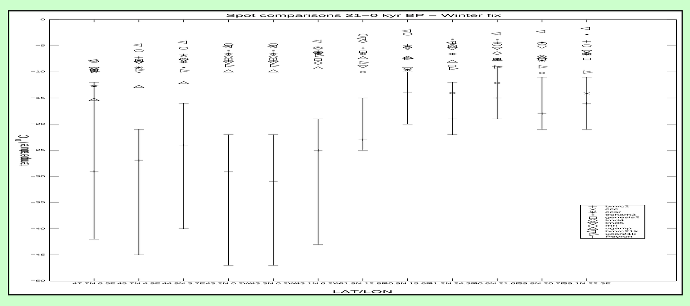


**Figure 6** Model-proxy comparisons for 21-0 kyr BP January temperature.

| | | 57N | 52N | 3.5W | 1.0W |
|---|---|---|---|---|---|
| January | Model | GENESIS2 | HADAM2 | GISS | LMD5 |
| | $r^2$ | 0.97 | 0.99 | 0.82 | 0.65 |
| | detrended $r^2$ | 0.81 | 0.47 | 0.68 | 0.56 |
| | rmse / °C | 2.0 | 1.3 | 1.7 | 1.7 |
| | detrended rmse / °C | 0.8 | 0.5 | 1.1 | 1.1 |
| July | Model | GISS | GENESIS2 | CCM36k | CSIRO |
| | $r^2$ | 0.94 | 0.95 | 0.97 | 0.93 |
| | detrended $r^2$ | 0.85 | 0.64 | 0.78 | 0.45 |
| | rmse / °C | 0.8 | 0.5 | 1.1 | 1.3 |
| | detrended rmse / °C | 0.6 | 0.4 | 0.9 | 1.0 |

**Table 2** A summary of the 'best' models for the present day (Model vs New *et al*. (1999)).

## 3. Transect selection

A transect is required for each month and time slice for downscaling. Four methods to find this transect are explored, with an example of the results for January given in **Table 3**:

| January | | | | | |
|---|---|---|---|---|---|
| **Statistics for best model method.** | **New vs best model.** | | | | |
| | **57N** | **52N** | **-3.5E** | **1.0E** | **Average** |
| Model | GENESIS2 | HADAM2 | GISS | LMD5 | |
| Correlation coefficients of original data. | **0.97** | **0.99** | 0.82 | 0.65 | 0.86 |
| Correlation coefficients of the detrended data | 0.81 | 0.47 | 0.68 | 0.56 | 0.63 |
| RMSE | 2.0 | 1.3 | **1.7** | **1.7** | **1.7** |
| Detrended RMSE | 0.8 | 0.5 | 1.1 | **1.1** | 0.9 |
| **Statistics for best model group method.** | **New vs best average of GISS, CCM36k and HADAM2 models.** | | | | |
| | **57N** | **52N** | **-3.5E** | **1.0E** | **Average** |
| Correlation coefficients of original data. | **0.97** | **0.99** | **0.84** | **0.68** | **0.87** |
| Correlation coefficients of the detrended data | **0.83** | **0.53** | **0.74** | 0.56 | **0.67** |
| RMSE | **1.7** | **1.1** | 1.9 | 2.0 | **1.7** |
| Detrended RMSE | **0.7** | **0.4** | **1.0** | **1.1** | **0.8** |
| | **New vs next best average of CCC, GENESIS2, GENESIS2c and HADAM2c models.** | | | | |
| | **57N** | **52N** | **-3.5E** | **1.0E** | **Average** |
| Correlation coefficients of original data. | **0.97** | **0.99** | 0.83 | 0.55 | **0.84** |
| Correlation coefficients of the detrended data | 0.77 | 0.61 | 0.71 | 0.39 | **0.62** |
| RMSE | 1.8 | 1.3 | 2.3 | 2.3 | **1.9** |
| Detrended RMSE | 0.9 | **0.4** | **1.0** | 1.2 | **0.9** |
| **Statistics for the simple average method.** | **New vs simple average.** | | | | |
| | **57N** | **52N** | **-3.5E** | **1.0E** | **Average** |
| Correlation coefficients of original data. | **0.97** | **0.99** | 0.81 | 0.49 | 0.81 |
| Correlation coefficients of the detrended data | 0.79 | 0.27 | 0.69 | 0.21 | 0.49 |
| RMSE | 2.1 | 1.3 | 2.2 | 2.1 | 1.9 |
| Detrended RMSE | 0.8 | 0.5 | 1.1 | 1.3 | 0.9 |
| **Statistics for the weighted average method.** | **New vs weighted average.** | | | | |
| | **57N** | **52N** | **-3.5E** | **1.0E** | **Average** |
| Correlation coefficients of original data. | 0.95 | **0.99** | 0.75 | 0.58 | 0.82 |
| Correlation coefficients of the detrended data | 0.63 | 0.46 | **0.74** | **0.58** | 0.60 |
| RMSE | 2.3 | **1.1** | **1.7** | **1.7** | **1.7** |
| Detrended RMSE | 1.4 | 0.5 | 1.4 | 1.3 | 1.2 |

**Table 3** Results from the 4 exploratory methods for choosing a best transect for downscaling. An example for present-day January temperature.

**Best model** – a best model is identified by k-means analysis for the present day. Produces the best results but cannot be applied to the other time slices due to there not being a model that performs well for all transects and months (**Table 2**).

**Best model group average** – a best group of models identified by k-means cluster analysis for the present day and the transects of this group are averaged. This group can be used for other time slices.

**Weighted average of models** – weightings defined by model complexity.

**Simple average** of all model transects.

The best model group average method was chosen. Polynomials were fitted to the resulting transects using an objective method (minimising the sum of the squared errors per degree of freedom) (**Figure 7**).

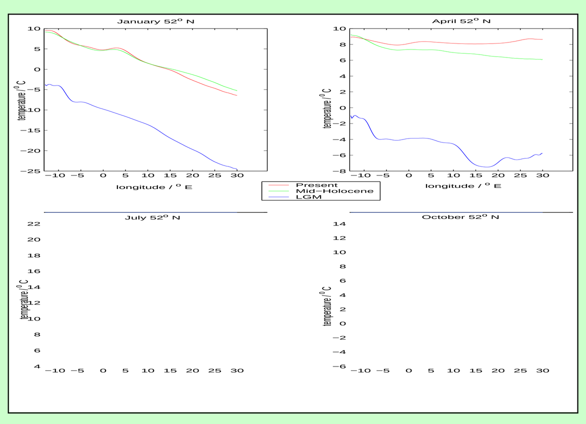


**Figure 7** Chosen transects for 52N.

## 4. Downscale from an EMIC

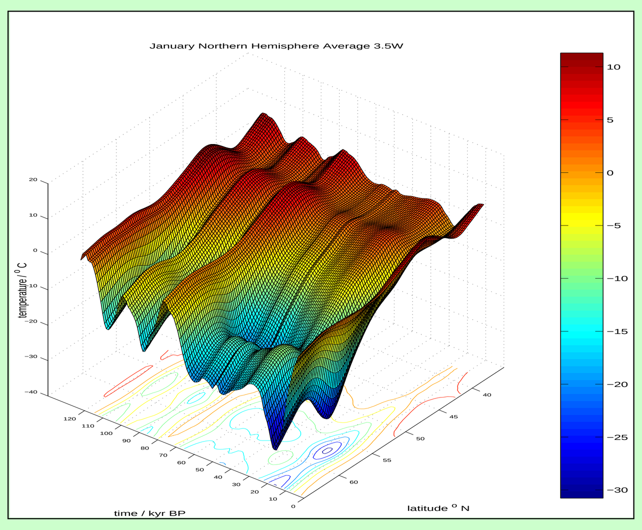


**Figure 8** Downscaled surface air temperature for 3.5W based on LLN2-D output.

LLN2-D is chosen to be the most suitable model to drive the downscaling procedure. The selection of this model over other models from UCL was based on ice volume evidence (**Figure 10**). Temperature fluctuations are too low in LLN2-D, and hence the LLN2-D northern hemisphere temperature output was linearly stretched to fit the observed present day data at one extreme and the best GCM data for the Last Glacial Maximum (LGM) at the other extreme. A scaling procedure was then applied to link the transects to these data to produce a downscaled data set (**Figure 8**).

The downscaled data have been extensively validated against proxy data both temporally and spatially. **Figure 9** compares a downscaled central England temperature against proxy data.

Agreement is good, although LLN2-D is too poorly resolved in time to reproduce the high frequency fluctuations that characterise the deglaciation.

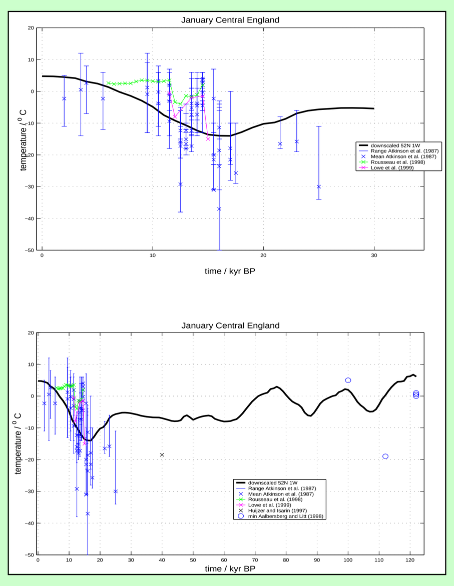


**Figure 9** Validation of downscaled central England temperature with proxy data.

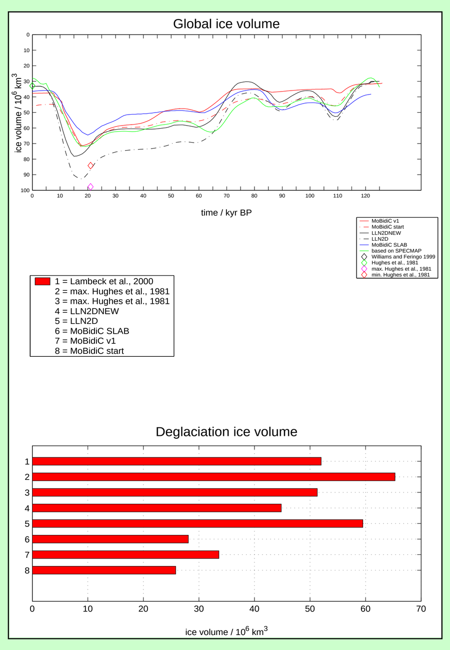


**Figure 10** Comparison of the results from 5 experiments made with LLN2-D and MoBiDiC. Global ice volumes and deglaciation ice volume amounts are shown.

References

Aalbersberg, G. and T. Litt, Multiproxy climate reconstructions for the Eemian and Early Weichselian., *Journal of Quaternary Science*, **13**, 367-390, 1998.
Atkinson, T. C., K. R. Briffa, and G. R. Coope, Seasonal temperatures in Britain during the past 22,000 years, reconstructed using beetle remains, *Nature*, **325**, 587-592, 1987.
Cheddadi, R., G. Yu, J. Guiot, S. P. Harrison, and I. C. Prentice, The climate of Europe 6000 years ago, *Climate Dynamics*, **13**, 1-9, 1997.
Hughes, T., G. Denton, B. Anderson, D. Schilling, J. Fastook, and C. Lingle, The last great ice sheets: a global view., in *The Last Great Ice Sheets*, edited by G. Denton and T. Hughes,John Wiley and Sons, New York, 1981.
Huijzer, A. S. and R. F. B. Isarin, The reconstruction of past climates using multi-proxy evidence: An example of the Weichselian pleniglacial in northwest and central Europe, *Quaternary Science Reviews*, **16**, 513-533, 1997.
Lambeck, K., Y. Yokoyama, P. Johnston, and A. Purcell, Global ice volumes at the Last Glacial Maximum and early late glacial, *Earth Planetary Science Letters*, **181**, 513-527, 2000.
Lowe, J. J., H. H. Birks, S. J. Brooks, G. R. Coope, D. D. Harkness, F. E. Mayle, C. Sheldrick, C. S. M. Turney, and M. J. C. Walker, The chronology of the palaeoenvironmental changes during the last glacial-Holocene transition: towards an event stratigraphy for the British Isles, *Journal of the Geological Society*, **156**, 397-410, 1999.
New, M., M. Hulme, and P. Jones, Representing Twentieth-Century Space-Time Climate Variability. Part I: Development of a 1961-90 Mean Monthly Terrestrial Climatology., *Journal of Climate*, **12**, 829-856, 1999.
Peyron, O., J. Guiot, R. Cheddadi, P. E. Tarasov, M. Reille, J.-L. De Beulieu, S. Bottema, and V. Andrieu, Climatic reconstructions in Europe for 18,000 yr BP from pollen data, *Quaternary Research*, **49**, 183-196, 1998.
Rousseau, D.-D., R. Preece, and N. Limondin-Lozouet, British late glacial and Holocene climatic history reconstructed from land snail assemblages, *Geology*, **26**, 651-654, 1998.
Williams, R. S. and J. G. Feringo, Introduction (US Geological Survey Professional Paper 1386-A), in *Satellite Image Atlas of Glaciers of the World*, edited by R. S. Williams and J. G. Feringo, 1999.

Acknowledgements

I would like to thank: the Palaeoclimate Modelling Intercomparison Project (PMIP) for making the data from their experiments available; Marie-France Loutre and Michel Crucifix for supplying data from experiments with LLN2-D and MoBidiC; Gerard Aalbersberg, Anna Broström, Rachid Cheddadi, Ruth Doherty, Chris Hewitt, Phil Jones, Akio Kitoh, Samuel Levis, Odile Peyron and Ulrike Wyputta for providing me with GCM and proxy data sets. This work was funded by Nirex UK ltd.

Mark Hoar
Climatic Research Unit
+44 (0)1603 592 702

m.hoar@uea.ac.uk
www.cru.uea.ac.uk

Climatic Research Unit
University of East Anglia
Norwich
NR4 7TJ